Int. J. Solids Structures Vol. 31, No. 2, pp. 219–230, 1994
Printed in Great Britain

0020-7683/94 $6.00+ .00

ANALYSIS OF PLASTIC BUCKLING OF RECTANGULAR STEEL PLATES SUPPORTED ALONG THEIR FOUR EDGES

TETSURO INOUE
Institute of Engineering Mechanics, University of Tsukuba, Tsukuba, Japan

(*Received* 27 *February* 1993; *in revised form* 2 *August* 1993)

Abstract—Plasticity in steel is characterized by an appreciable amount of plastic flow (in the yield plateau range) which precedes strain-hardening. This study is devoted to an analytical evaluation of plastic buckling stress of uniformly compressed rectangular steel plates, supported along their four edges, by the use of a modulus in shear and bending stiffnesses derived by the author (Inoue and Kato, 1993, *Int. J. Solids Structures*, **30**, 835–856) based on the Tresca yield criterion. Their values were analytically derived by the concept that plastic strain is to be caused by slip. In this paper, analytical results are compared with those tested by the author, and the former are in good agreement with the latter especially in the early plastic zone.

1. INTRODUCTION

Various researches have been made for plastic buckling of plates. These were summarized by the author (Inoue and Kato, 1993).

The discrepancy between theoretical value and test result is going to be diminished. However theory is not able to explain this problem perfectly yet. The author (Inoue and Kato, 1993) previously obtained equivalent plastic shear modulus and bending stiffnesses of steel plate under compression at the instant of buckling whose material is characterized by plastic-flow and strain-hardening. And these values were applied to the buckling analysis of a cruciform section column. In its analysis, analytical results were shown to be in good agreement with the first test in the early plastic zone. In its analysis, yielding of a steel plate was to follow the Tresca yield criterion. Plastic deformation of the plate was to be caused by slips which develop only in the directions of maximum shear stress. Its analysis concretely investigated a nonuniform distribution of slips depending on the orientation of an infinite number of possible slip planes at each point in the plate. As a result, equivalent shear modulus was equal to half the elastic shear modulus everywhere in the plastic range, and all the bending stiffnesses vanished in the plastic-flow range. In the strain-hardening range, the equivalent shear modulus was again equal to half of the elastic value and one bending stiffness in the x-direction was nonzero. The reason why the equivalent shear modulus had such a low value is that, in the plastic range, simple shear plastic deformation in the transverse cross-section is created at the instant of plate buckling and the exerted elastic shear strain is much less. In this paper, these moduli and stiffnesses are applied to the plastic buckling analysis of rectangular steel plates under compression supported along their four edges. These results are compared with test results carried out by the author.

2. PLASTIC BUCKLING OF STEEL PLATES SUPPORTED ALONG THEIR FOUR EDGES UNDER UNIAXIAL COMPRESSION

2.1. *Shear modulus and bending stiffnesses*

A steel plate supported along its four edges under uniaxial compression is shown in Fig. 1. In this figure, d is plate width, σ is working stress.

The bending and torsional moments of an orthogonally anisotropic plate are given by the following equations (Girkmann, 1956):

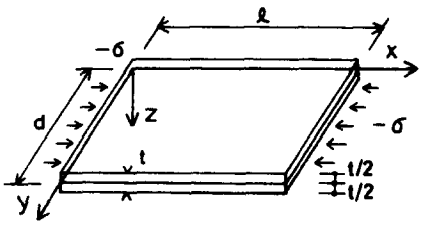

Fig. 1. Plate and working stress.

$$\left.\begin{aligned} M_x &= D_x I\phi_x + D_{xy} I\phi_y \\ M_y &= D_y I\phi_y + D_{yx} I\phi_x \\ M_{xy} &= 2G_p I\phi_{xy} \end{aligned}\right\}, \tag{1}$$

where

M_x: bending moment around y-axis per unit width
M_y: bending moment around x-axis per unit width
M_{xy}: torsional moment per unit width
D_xI, D_yI, $D_{xy}I$, $D_{yx}I$: bending stiffnesses
G_pI: torsional stiffness
G_p: shear modulus
$I = t^3/12$

$\phi_x = -\dfrac{\partial^2 w}{\partial x^2}$: curvature in x-direction

$\phi_y = -\dfrac{\partial^2 w}{\partial y^2}$: curvature in y-direction

$\phi_{xy} = \dfrac{\partial^2 w}{\partial x\,\partial y}$: twist of the surface with respect to the x- and y-axes

w: out-of-plane displacement (displacement ion z-direction).

The author (Inoue and Kato, 1993) showed that G_p, D_x, D_y, D_{xy}, D_{yx} took the following value:

(plastic-flow range)

$$G_p = \tfrac{1}{2}G, \tag{2}$$

where

$G = \dfrac{E}{2(1+\nu)}$: elastic shear modulus

$E = 205940\ \mathrm{N\ mm^{-2}}$: Young's ratio
$\nu = 0.3$: Poisson's ratio of steel.

$$D_x = D_y = D_{xy} = D_{yx} = 0. \tag{3}$$

(Strain-hardening range)

$$G_p = \tfrac{1}{2}G \tag{2}'$$

$$\left.\begin{aligned} D_x &= E_{st} \\ D_y &= D_{xy} = D_{yx} = 0 \end{aligned}\right\}, \tag{4}$$

where

E_{st}: tangent modulus on the stress–strain curve of the material in the strain-hardening range.

2.2. *Buckling analysis*

The equilibrium equation of the plate at buckling is given as follows:

$$\frac{\partial^2 M_x}{\partial x^2} - 2\frac{\partial^2 M_{xy}}{\partial x\,\partial y} + \frac{\partial^2 M_y}{\partial y^2} = N\frac{\partial^2 w}{\partial x^2}, \tag{5}$$

where

$N = \sigma_{cr} t$: bifurcation strength per unit width
σ_{cr}: bifurcation stress.

(Plastic-flow range)

Substituting eqns (2), (3) for eqns (1) and applying to eqn (5), I obtain

$$\frac{\partial^4 w}{\partial x^2\,\partial^2 y} + \frac{N}{2GI}\frac{\partial^2 w}{\partial x^2} = 0. \tag{6}$$

The out-of-plane displacement is assumed as:

$$w = f(y)g(x). \tag{7}$$

Substituting eqn (7) for eqn (6), I obtain

$$\ddot{g}(x)\left[f''(y) + \frac{N}{2GI}f(y)\right] = 0, \tag{8}$$

where $\cdot$ and $''$ indicate derivatives with respect to x and y, respectively. The boundary conditions are represented by

$$\left.\begin{aligned} g(x) &= 0 \quad \text{at} \quad x = 0, l \\ f(y) &= 0 \quad \text{at} \quad y = 0, d \end{aligned}\right\}. \tag{9}$$

Equation (8) is satisfied by the following two relations: $\ddot{g}(x) = 0$ or $f''(y) + (N/2GI)f(y) = 0$. Considering the boundary conditions at $x = 0$ and l, the former relation reduces to $g(x) = 0$, or $w = 0$ which is a trivial solution representing no buckling. The general solution for the latter relation is given by

$$f(y) = A\sin\sqrt{\frac{N}{2GI}}y + B\cos\sqrt{\frac{N}{2GI}}y. \tag{10}$$

From the boundary condition at $y = 0$, I obtain

$$f(y) = A\sin\sqrt{\frac{N}{2GI}}y. \tag{11}$$

Thus

$$w = A\sin\sqrt{\frac{N}{2GI}}y\cdot g(x). \tag{12}$$

From the boundary condition at $y = d$, I obtain

$$\sin\sqrt{\frac{N}{2GI}}d = 0. \tag{13}$$

Thus

$$\sqrt{\frac{N}{2GI}}d = \pi. \tag{14}$$

Finally, the following bifurcation strength and stress are obtained:

$$\left.\begin{aligned} N &= \frac{2\pi^2}{d^2}GI \\ \sigma_{cr} &= \frac{\pi^2}{6}G\left(\frac{t}{d}\right)^2 \end{aligned}\right\}. \tag{15}$$

The function $g(x)$ is required to satisfy the boundary conditions $g(0) = g(l) = 0$, but is otherwise arbitrary.

Substituting N expressed by eqns (15) for eqn (11), the mode of buckling wave in the direction of the plate width is obtained as:

$$f(y) = A\sin\frac{\pi}{d}y. \tag{16}$$

The boundary conditions (9) hold identically for the conditions, simply supported and fixed at edges $y = 0$ and d. So bifurcation solutions for both the above conditions are identically given by eqns (15).

(Strain-hardening range)

Substituting eqns (2)′, (4) for eqns (1) and applying to eqn (5), I obtain

$$E_{st}I\frac{\partial^4 w}{\partial x^4} + 2GI\frac{\partial^4 w}{\partial x^2\,\partial y^2} + N\frac{\partial^2 w}{\partial x^2} = 0. \tag{17}$$

The out-of-plane displacement is assumed as eqn (7) and substituting to eqn (17), I obtain

$$E_{st}I\dddot{g}(x)f(y) + 2GI\ddot{g}(x)f''(y) + N\ddot{g}(x)f(y) = 0. \tag{18}$$

When both edges are simply supported at $x = 0$ and l, adding the condition $\ddot{g}(x) = 0$ at $x = 0$ and l to the boundary conditions given by eqn (9) and solving eqn (18) using the method of separation variables, I obtain

$$g(x) = A\sin\frac{m\pi}{l}x. \tag{19}$$

Then,

$$f''(y) + \frac{1}{2GI}\left(N - \frac{m^2\pi^2}{l^2}E_{st}I\right)f(y) = 0. \tag{20}$$

Equation (20) is rewritten as

$$\left.\begin{aligned} &f''(y)+Hf(y)=0 \\ &H=\frac{1}{2GI}\left(N-\frac{m^2\pi^2}{l^2}E_{st}I\right) \end{aligned}\right\}. \tag{21}$$

The general solution of eqn (21) when $H \neq 0$ is given by

$$f(y) = B\sin\sqrt{H}y + C\cos\sqrt{H}y. \tag{22}$$

The boundary conditions are given by eqn (9). Thus, from the condition at $y = 0$

$$f(y) = B\sin\sqrt{H}y. \tag{23}$$

Thus the buckling mode is represented by

$$w = AB\sin\sqrt{H}y \cdot \sin\frac{m\pi}{l}x. \tag{24}$$

From the boundary condition at $y = d$, I obtain

$$\sin\sqrt{H}d = 0. \tag{25}$$

Namely

$$\sqrt{H}d = \pi. \tag{26}$$

Therefore the following bifurcation strength is obtained:

$$N = \frac{2\pi^2}{d^2}GI + \frac{m^2\pi^2}{l^2}E_{st}I. \tag{27}$$

N defined by eqn (27) is minimum at $m = 1$. Thus, I obtain the following bifurcation strength and stress:

$$\left.\begin{aligned} N &= \frac{2\pi^2}{d^2}GI + \frac{\pi^2}{l^2}E_{st}I \\ \sigma_{cr} &= \frac{\pi^2}{12}\left[2G+\left(\frac{d}{l}\right)^2 E_{st}\right]\left(\frac{t}{d}\right)^2 \end{aligned}\right\}. \tag{28}$$

Assuming $H = 0$ in eqn (21), I obtain $f(y) = Dy$ which represents a linear mode in the direction of the plate width, but considering the boundary condition at $y = 0, d$, it is noticed that this solution results in $f(y) = 0$, that is, a trivial one of no buckling.

Comparing eqns (28) with eqns (15) which were derived for plastic flow range, eqns (28) give higher solutions because of the difference in the second term including E_{st} in the first part of eqns (28). However the difference is at most 1.4% when $l/d = 1.5$ and $E/E_{st} = 40$.

Substituting H from eqn (26) in eqn (24) and selecting $m = 1$, the following buckling mode is obtained:

$$w = AB\sin\frac{\pi}{d}y\sin\frac{\pi}{l}x. \tag{29}$$

It is the same as the plastic-flow range that the bifurcation solutions are identical for both boundary conditions, simply supported and fixed, at $y = 0, d$.

2.3. *Comparison with cruciform section column*

The result of the present paper is compared with that of cruciform section column analytically derived by the author (Inoue and Kato, 1993).

The author showed that bifurcation stress and mode of buckling wave of cruciform section column were given as follows:

(plastic-flow range)

$$\sigma_{cr} = \frac{\pi^2}{24} G \left(\frac{t}{b}\right)^2, \tag{30}$$

where

b: projecting width of cruciform section column

$$w = A \sin \frac{\pi}{2b} y \cdot g(x). \tag{31}$$

(strain-hardening range)

$$\sigma_{cr} = \frac{\pi^2}{12} \left[\frac{G}{2} + E_{st} \left(\frac{b}{l}\right)^2\right] \left(\frac{t}{b}\right)^2, \tag{32}$$

$$w = AB \sin \frac{\pi}{2b} y \sin \frac{\pi}{l} x. \tag{33}$$

Comparing these bifurcation stresses with those derived in the present paper (eqn (15) in the plastic-flow range and eqn (28) in the strain-hardening range), the following distinguishing character becomes clear. Bifurcation stress of the steel plate supported along its four edges whose width d is $2b$ twice the projecting width of the cruciform section column, has the same value as that of the cruciform section column. As for the mode of the buckling wave, dividing the plate supported along its four edges into two parts along its center line in the longitudinal direction, the mode of each plate is equal to that of one plate which forms the cruciform section column. This feature is shown in Fig. 2 in the direction of the plate width. Conversely, if connecting two modes of plates, which form the cruciform section column, at their free edges, the obtained mode is the same as that of a plate supported along its four edges. In Fig. 2, (a) is the section before buckling, (b) is the mode after buckling of the plate supported along its four edges, and (c) is the process to divide into two parts. The dashed lines which divide the section into sub-sections remain parallel after buckling of the original lines before buckling. The reason that this feature takes place is as follows:

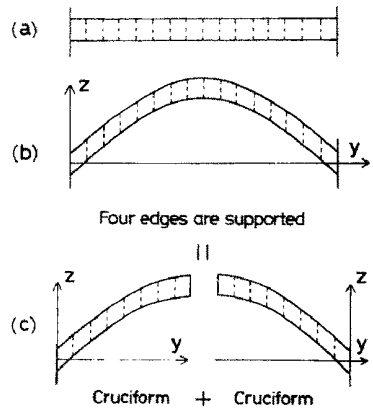

Fig. 2. Buckling mode.

The general solutions for the mode of buckling wave in the direction of the plate width are represented by eqns (10) and (22) for buckling in the plastic flow range and in the strain hardening range, respectively. They must satisfy the boundary conditions given by eqn (9) which are valid both for simply supported edges and fixed edges at $y = 0$ and d. Therefore, these different support conditions have the same bifurcation stress and the same mode of buckling wave (sine wave in the direction of the plate width). As described by the author (Inoue and Kato, 1993), shear deformation in the transverse cross-section can take place at the instant of buckling accompanied by torsion. Thus, the buckling wave mode in the direction of the plate width satisfying the above-mentioned boundary conditions must be accompanied by the shear deformation as shown in Fig. 2.

The detailed study of the aspect of slip deformation of the plate which forms the cruciform section column holds in the same way for the present problem. This is because of the analogy mentioned above.

3. TEST AND ANALYTICAL RESULTS

A compression test of box-section steel stub-columns was conducted as representative of the plates supported along their four edges.

3.1. *Test program*

The specimens are welded box-section stub-columns as shown in Fig. 3. The corner joint was formed by a partial penetration weld applying single V groove with 1 mm root face. The ends of the stub-columns were milled plane and perpendicular to the longitudinal axis of the stub-columns. The weld reinforcement was removed by a grinder. After completion of welding and mechanical finishing, the specimens were annealed, in which specimens' temperature was kept at 600°C for an hour and then slowly cooled in a heat treatment furnace.

The material of the stub-columns is mild steel designated by SS400 in JIS. The measured thickness of the plate elements was 5.81 mm. The measured dimensions of the specimens are shown in Table 1. The total number of the specimens is 22, and they are classified as Series A and B. The specimens of Series A and B are distinguished by the value of L/d, i.e. $L/d = 1.5$ for Series A and $L/d = 3.0$ for series B.

It is usually suitable to make specimens as long as possible unless column buckling takes place in order to obtain lowest buckling strength of plates. The length $l/d = 3$ is frequently adopted in this type of stub-column specimen in a compression test. Column buckling does not take place in these specimens. The reason why more shorter specimens, $l/d = 1.5$, are planned is to examine the effect of the length of the specimens.

The definition of symbols in Table 1 is as follows:

t: thickness of the plate
d: width of the section
L: length of the specimen
d/t: width-to-thickness ratio.

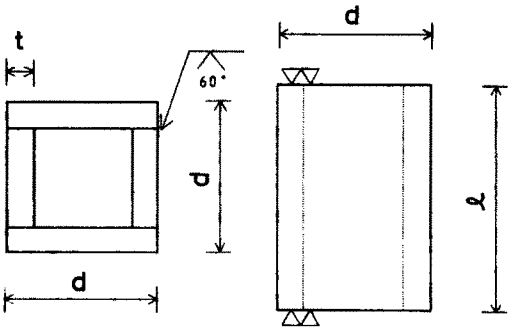

Fig. 3. Specimens.

Table 1. Specimens of stub-column test

Code	d (mm)	l (mm)	d/t	l/d
A-10	58.00	87.0	10	1.5
A-12	69.55	104.4	12	1.5
A-14	81.25	121.8	14	1.5
A-16	92.75	139.2	16	1.5
A-18	104.45	156.2	18	1.5
A-20	116.05	174.0	20	1.5
A-22	127.60	191.4	22	1.5
A-24	139.15	208.8	24	1.5
A-26	150.85	226.2	26	1.5
A-28	162.45	243.6	28	1.5
A-30	174.15	261.0	30	1.5
B-10	57.90	174.0	10	3.0
B-12	69.55	208.8	12	3.0
B-14	81.25	243.6	14	3.0
B-16	93.00	278.4	16	3.0
B-18	104.45	313.2	18	3.0
B-20	115.90	348.0	20	3.0
B-22	127.75	382.8	22	3.0
B-24	139.20	417.6	24	3.0
B-26	150.90	452.4	26	3.0
B-28	162.45	487.0	28	3.0
B-30	174.05	522.0	30	3.0

The mechanical property of the material from tension test is shown in Fig. 4 and Table 2. The definition of symbols in the figure and table is shown as follows:

σ_Y: yield stress
σ_m: maximum stress
ε_Y: yield strain (σ_y/E)
ε_{st}: strain at the onset of strain-hardening
E_{st}: strain-hardening modulus.

These values were different from compression test of stub-columns. The property from the compression test is shown in Table 3. The definition of symbols in the Table is shown as follows:

${}_c\bar{\sigma}_Y$: average yield stress
${}_c\bar{\varepsilon}_Y$: average yield strain (${}_c\bar{\sigma}_Y/E$)
${}_c\bar{\varepsilon}_{st}$: average strain at the onset of strain-hardening
${}_c\bar{E}_{st}$: representative value of tangent modulus in the strain-hardening range (value of the specimen A-10 which has the smallest value of d/t).

3.2. *Test procedure*

3.2.1. *Loading method.* Load was centrally and monotonically applied using 200-ton screw type testing machine. The specimens were placed on a thick steel plate designated by

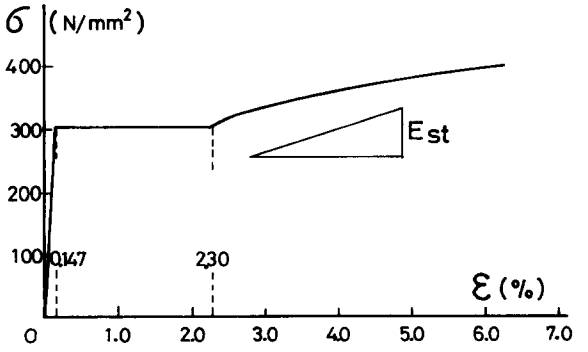

Fig. 4. Stress–strain curve.

Table 2. Mechanical properties from tension test

Material	σ_Y (N mm^{-2})	σ_m (N mm^{-2})	σ_Y/σ_m	ε_Y (%)	ε_{st} (%)	$\varepsilon_{st}/\varepsilon_Y$	E_{st} (N mm^{-2})	E_{st}/E
SS400	304	445	0.683	0.147	2.30	15.6	3805	0.0185

Table 3. Mechanical properties from compression test

Material	${}_c\bar{\sigma}_Y$ (N mm^{-2})	${}_c\bar{\varepsilon}_Y$ (%)	${}_c\bar{\varepsilon}_{st}$ (%)	${}_c\bar{\varepsilon}_{st}/{}_c\bar{\varepsilon}_Y$	${}_c\bar{E}_{st}$ (N mm^{-2})	${}_c\bar{E}_{st}/E$
SS400	318	0.154	1.27	8.26	4491	0.0218

A in Fig. 5 and the plate A was placed on a steel base with sufficient strength and rigidity. Load was applied through a bearing plate B. Plates C were attached in order to measure axial shortening after mentioned. At the beginning of loading, the bearing plate B was kept free to rotate. After visually confirming the perfect contact between the bearing plate and the top-face of the specimen, the bearing plate was fixed using nuts and bolts to prevent rotation.

3.2.2. *Measurement of deformation.* Axial shortening between plates C was measured by four dial gages as shown in Fig. 5. Measuring positions are four positions on the continuation of diagonal lines of the section of the specimen.

3.3. *Test results*

3.3.1. *Load–deformation relation.* $\sigma/{}_c\sigma_Y$–$\varepsilon/{}_c\varepsilon_Y$ relations were obtained as test results. These are relations between the following two nondimensionalized volumes. One is working stress σ divided by the yield stress ${}_c\sigma_Y$, and the other is strain ε, axial shortening divided by the length of the specimen, divided by the yield strain ${}_c\varepsilon_Y$. Test results showed clear plastic-flow. These results are shown in Figs 6(a, b). Termination of curves in these figures are breaking points of welded parts.

3.3.2. *Stress increase and analytical value.* Nondimensionalized stress increases rate τ, and the experimentally obtained maximum stress σ_{max} divided by ${}_c\sigma_Y$, are shown in Table 4. These are graphically shown in Fig. 7. In Fig. 7, the ordinate is the stress increase rate τ, and the abscissa is equivalent to the width-to-thickness ratio $d/t\sqrt{{}_c\bar{\varepsilon}_Y}$. I compare these

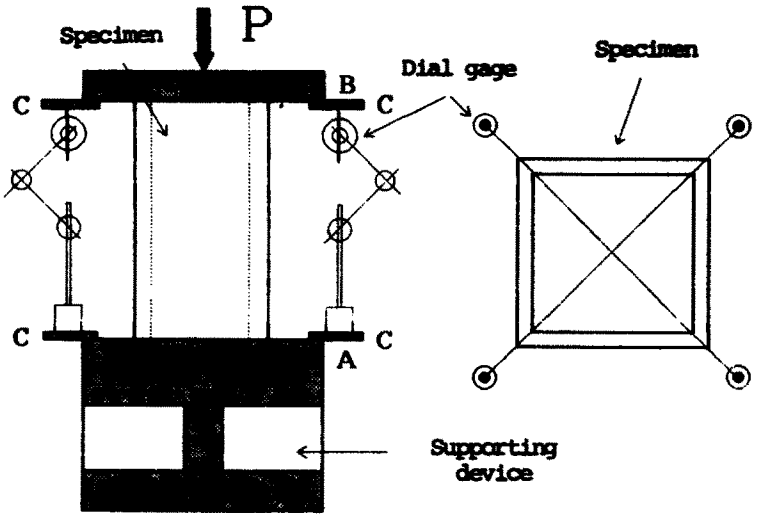

Fig. 5. Test set-up.

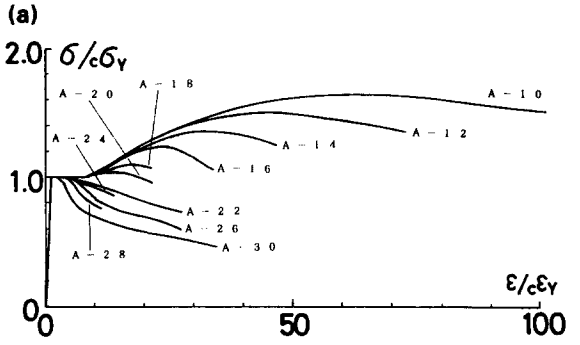

Fig. 6(a). $\sigma/_c\sigma_Y - \varepsilon/_c\varepsilon_Y$ curve for series A.

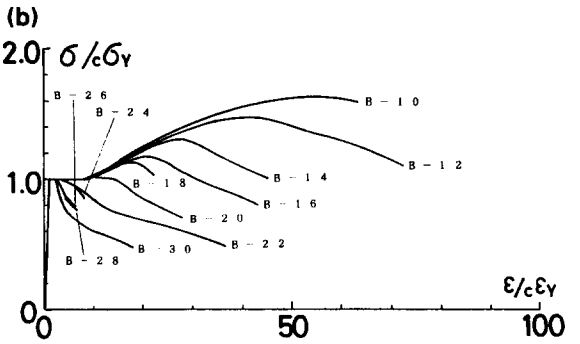

Fig. 6(b). $\sigma/_c\sigma_Y - \varepsilon/_c\varepsilon_Y$ curve for series B.

τs with the analytical values obtained in Section 2. For comparison, eqn (15) in Section 2 for the plastic-flow range is used because eqn (28) for strain-hardening range is almost the same as in eqn (15).

Dividing both sides of eqn (15) by the yield stress σ_Y:

$$\frac{\sigma_{cr}}{\sigma_Y} = \frac{\pi^2}{12(1+\nu)} \frac{1}{(d/t\sqrt{\varepsilon_Y})^2}. \tag{34}$$

Supposing the left-hand side of the above equation is equal to τ, this equation is drawn

Table 4. Test results

Code	τ	$d/t\sqrt{{}_c\varepsilon_Y}$
A-10	1.65	0.392
A-12	1.51	0.471
A-14	1.36	0.549
A-16	1.24	0.628
A-18	1.10	0.706
A-20	1.05	0.785
A-22	1.00	0.863
A-24	1.00	0.942
A-26	1.00	1.020
A-28	1.00	1.099
A-30	1.00	1.177
B-10	1.63	0.392
B-12	1.47	0.471
B-14	1.31	0.549
B-16	1.18	0.628
B-18	1.13	0.706
B-20	1.01	0.785
B-22	1.00	0.863
B-24	1.00	0.942
B-26	1.00	1.020
B-28	1.00	1.099
B-30	1.00	1.177

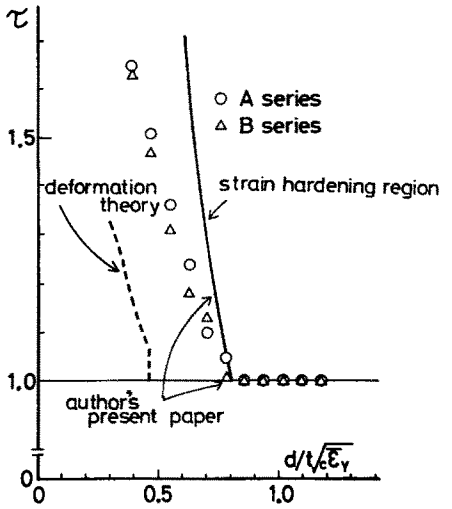

Fig. 7. Analytical and test results.

by a solid line in Fig. 7. Equation (15) for the plastic-flow range is originally significant at one point at which eqn (15) intersects the line defined by $\sigma = \sigma_Y$. So this point is that at which eqn (34) intersects the line defined by $\tau = 1.0$ in Fig. 7. The analytical solution for the strain-hardening range is nearly equal to the increasing part of eqn (34) beyond 1.0 as mentioned above.

The minimum solutions derived from deformation theory by Stowell and Pride (1951) on the basis of Fig. 4 are also shown in Fig. 7 by a dashed line. These solutions are derived for the long plates simply supported along all four edges.

This figure demonstrates that the analysis and the experiment have exceptional agreement with respect to the upper limit of the width-to-thickness ratio range in which axial stress can be increased over the yield stress into the strain-hardening range.

With the decrease in the effective width-to-thickness ratio in the strain-hardening range, the stress increase rate becomes larger, but the experimental data points are below the analytical predictions. The reason for this discrepancy is not apparent, but may be due to the loss of geometric similarity of the yield locus in the strain-hardening range, which is the basic assumption in this analysis. When the geometric similarity is impaired, slip deformations in different directions can be combined.

It can be concluded that the proposed analytical method provides a good agreement with the experimental results especially in the early plastic zone.

4. SUMMARY AND CONCLUSIONS

Plastic buckling of steel plates supported along their four edges was analysed, and the results were compared with test results. The main points of this paper are as follows:

(1) Shear modulus and bending stiffnesses obtained by the authors (Inoue and Kato, 1993) are used in the analysis of plastic buckling of rectangular steel plates supported along their four edges under uniaxial compression.
(2) Bifurcation stress of the steel plate supported along its four edges whose width d is $2b$, twice the projecting width of the cruciform section column, has the same value as that of the cruciform section column.
(3) As for the mode of buckling wave, dividing the plate supported along its four edges into two parts along its center line in the longitudinal direction, the mode of each plate is equal to that of one plate which forms the cruciform section column.
(4) The detailed study, by the author (Inoue and Kato, 1993), of the aspect of slip deformation in the section of the plate which forms the cruciform section column holds in the same way for the present problem. This is because of the analogy of Conclusions (2), (3).

(5) For buckling in the plastic-flow range, the buckling wave mode in the longitudinal direction must satisfy the condition that the displacement at the boundary is equal to zero, but is otherwise arbitrary. For buckling in the strain-hardening range, the buckling mode in the longitudinal direction is sinusoidal. The buckling mode in the transverse direction is sinusoidal both for the plastic-flow and for the strain-hardening ranges.
(6) The analytically obtained width-to-thickness ratio to reach the onset of strain-hardening surprisingly coincides with the test result.
(7) With the decrease in the effective width-to-thickness ratio in the strain-hardening range, the stress increase rate obtained experimentally is below the analytical predictions.
(8) Proposed analytical results provide a good agreement with test results especially in the early plastic zone.

REFERENCES

Girkmann, K. (1956). *Flachentragwerke*. Springer, Berlin.
Inoue, T. and Kato, B. (1993). Analysis of Plastic Buckling of Steel Plates. *Int. J. Solids Structures* **30**(6), 835–856.
Stowell, E. Z. and Pride, R. A. (1951). The effect of compressibility of the material on plastic buckling. *J. Aero. Sci.* **18,** 773.